Smart Geotechnics for Smart Societies – Zhussupbekov, Sarsembayeva & Kaliakin (Eds)

A sink hole and caves caused by earth balance shield and digital twin observational method to control face stability

Y. Iwasaki
Geo Research Institute, Kobe, Japan

H. Ito
JIP Techno Science, Osaka, Japan

Y. Koyama
Ritsumeikan University, Kyoto, Japan

A.Zh. Zhussupbekov
L.N. Gumilyov Eurasian National University, Nur Sultan, Kazakhstan

ABSTRACT: A sink hole was found at ground surface in a residential area in Tokyo in October 2020. The site was above a construction line of earth pressure balance shield tunnel with16.1 m in diameter and the crown at the depth of GL-47m. Further study revealed the dense sand layer above the tunnel has been loosened along the tunnel for about 200m length from the tunnel face.

3DFEM simulation based upon the site conditions showed a possibility of the loosing stability of the face when the ground is dense sand with little fine component.

A digital twin observational method is proposed to discuss the face stability and to keep digging safe.

1 UNEXPECTED ACCIDENT BY EARTH PRESSURE BALANCED SHIELD

1.1 *A sink hole above 47m of earth balanced pressure shield of 16.1m in diameter*

A sink hole was reported by East Nippon Expressway Co. Kanto Regional Head Office on October 18, 2020(ENE). A depression of ground surface appeared on a narrow road in front of a private house on Sunday around 12:30 October 18, 2020 in Chofu-city, Tokyo. It was reported the location was just above the tunneling site of the Tokyo Outer Ring Road (Tomei-Kan-etsu) main line tunnel (southbound). The size of the depression was 5m x 2.5m on the ground surface as shown "Sink hole" in Figure 1.

The shield had passed below the sink point with about 47m below the surface on September 14, 2020, about one month earlier than the sink hole appeared. Based upon razer scanning and seismic survey along the shield line, additional void zones were identified as shown in Figure 1.

1.2 *Loosening ground above the shield tunnel*

Based upon borings before the construction, the area was recognized as thick dense sand ground with a thin gravel layer of Pleistocene with SPT N>50 covered by alluvium soft loam Holocene layer.

After the sink was found, several borings were performed to study the geotechnical conditions. The depth distributions of the SPT, N values for these borings are shown in Figure 2. The

DOI: 10.1201/9781003299127-131

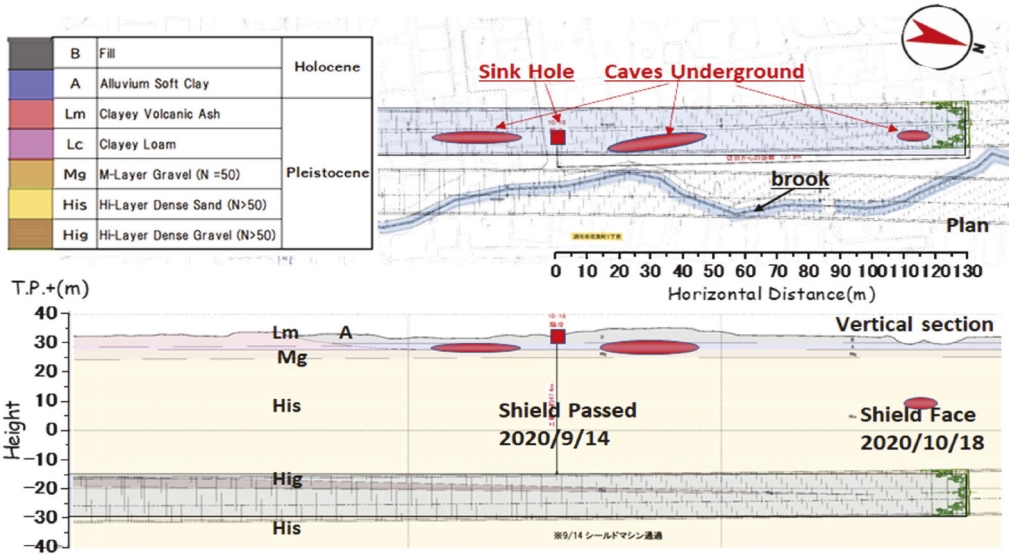

Figure 1. A sink hole and caves underground above a shield tunnel in Chofu-city, Tokyo.

N-values above the shield tunnel for the His Sand layer shows significantly decreased values compared to those before the construction. The N-values in the zone above the shield tunnel shows less than 50 (N<50) not only below the sink and the caves but also other points where no sink or cases was identified. The decreased N-values from N>50 to N<5-50 are found along the tunnel line of 200m from the face. The loosening of the dense sand ground above the shield tunnel was caused by tunneling and induced to create caves and sink holes just above the shield tunnel.

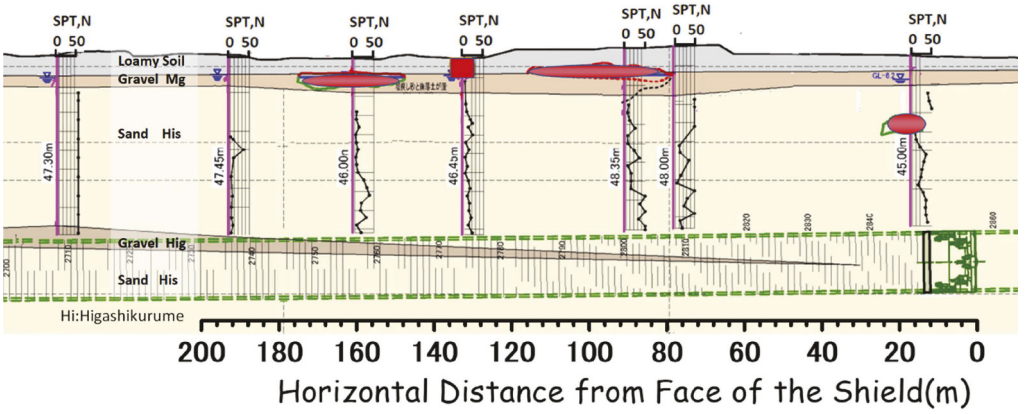

Figure 2. The loosened dense sand layer above the shield about 200m from the face.

1.3 *Chamber pressure*

To keep the stability of the face, the chamber pressure should be kept within some safety range as well as the mud in the chamber under liquid plastic state for the pressures to be distributed smoothly all over the face with a large diameter of 16.1 m.

Monitoring mud pressures in the chamber is a common practice in the earth balanced pressure tunneling. Figure 3 shows the position of the earth pressure sensors. Outer pressure sensors and inner pressure sensors were installed to monitor the chamber pressure.

Figure 4 shows earth pressure distribution near the face of shield machine. Distribution of pressures in front of the face consists of horizontal earth pressure σ_h and water pressure σ_w. On the other hand, the chamber pressure that should be balanced against the earth pressures.

1.4 *Monitored chamber pressure*

Monitored chamber pressures during the process of tunneling in the area where the sink surface and caves underground were found are plotted in Figure 5. Monitored data are found to be grouped into two types of digging and stopping phases.

The chamber pressures at the crown level are the same of the water pressure for both groups. The pressure increment with depth is 12 to 14 kN/m2 for digging phase, which is the same as the unit mass density of mud in the chamber. When the shield machine is under stopping phase, no mixing of the mud in chamber and the pressure increase with depth is the same as the density of water.

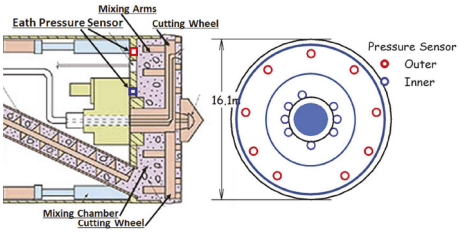

Figure 3. Positions of earth pressure sensors in chamber.

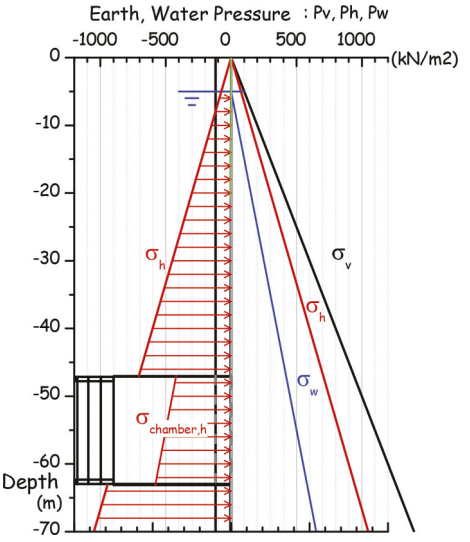

Figure 4. Earth and chamber pressures.

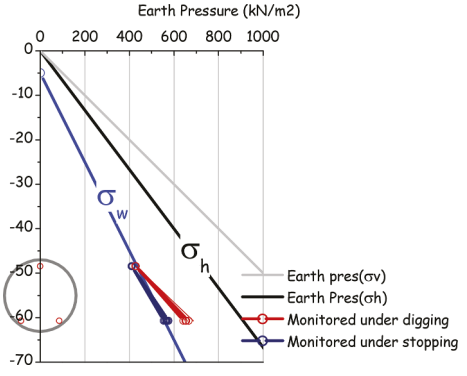

Figure 5. Monitored chamber pressures.

Table 1. Monitored chamber pressure.

Phase	Digging	Stopping
Pressure at crown(kN/m2)	38	38
dp/dz(kN/m3)	12~14	10

Water pressure at the crown = 42(kN/m2)

2 ESTIMATION OF FACE STABILITY

2.1 *Analytical model*

An analytical model for discussion of face stability of the pressure balanced shield of the site as 3D FEM model by Plaxis is shown in Figure 6. The half sectional model of the dimension of 200m in width, 100m in length, and 90m in depth.

2.2 *Properties of ground for analysis*

The ground at the level of the shield and about more than 30 m above the shield consists of dense sand or dense gravel formations of Hs and Hg which shows SPT, N>50. The internal friction angle of sand and gravel was proposed to have a relationship with SPT, N1 as shown in Figure 7 (Hatanaka). N1 is a function of SPT, N as follows,

$$N1 = N/\left(\sigma_v'/98\right)^{0.5}$$

The effective vertical stress at the mid-level of the face (d=55m) under water level of WL=GL-5m and unit mass of sand of 20kN/m3 is obtained as

$$N1 = 50/((20 \times 55 - 10 \times 50)/98)^{0.5} = 20.4$$

The internal friction angle is obtained as

$$\phi = 40^{o} \text{ for } N1 = 20.4$$

The cohesion of sand and gravel soil is a function of the contents of fine soil of clay and silt. The change of the grain size distributions which were obtained by soil test of the excavated mud soils is shown in Figure 8. The fine content of the sand layer in the loosened zone for dense sand above the shield is less than 7.5-5%. The relationship between the cohesion and the fine contents of sand and gravel soil (Kim) as shown in Table 2. The estimated cohesion is around C' = 0 (kN/m2).

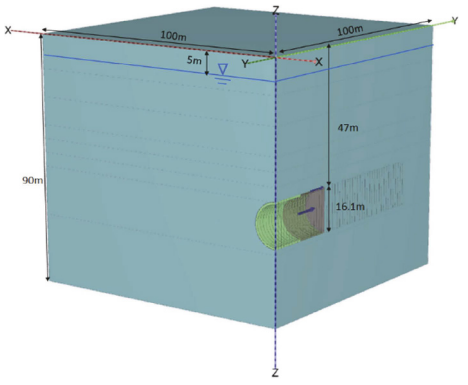

Figure 6. FEM model.

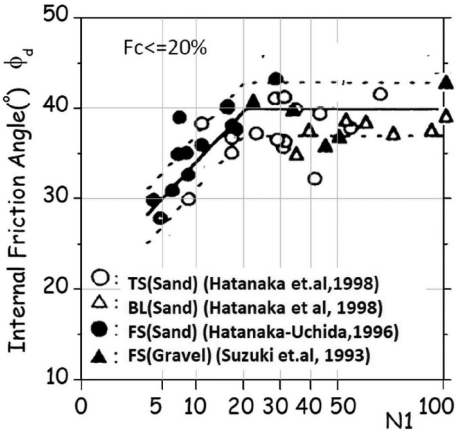

Figure 7. Relationship between N1 and friction angle.

2.3 *3D FEM simulation on face stability for stopping phase*

The force of the shield machine against the face is the sum of the thrust force and the chamber pressure. During the stopping phase of installing of tunnel segments after digging 1.6m of the

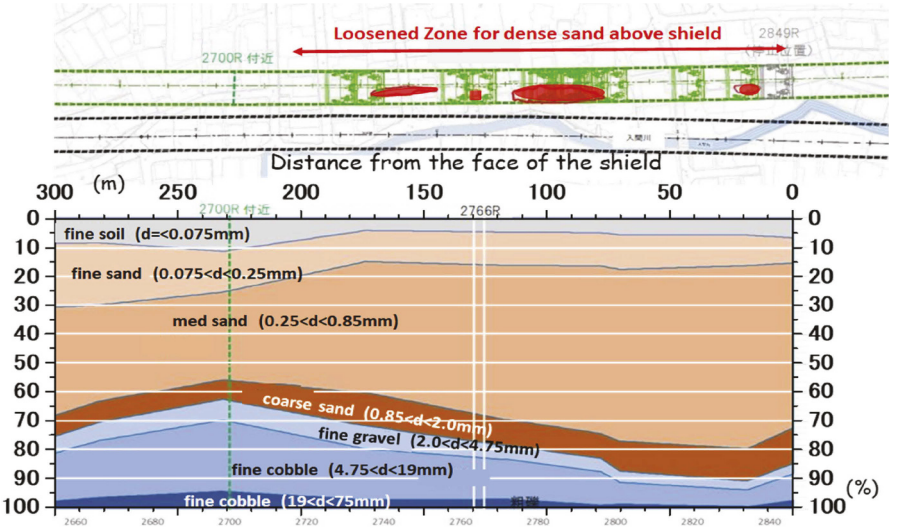

Figure 8. Change of the grain size distribution of the excavated mud.

Table 2. Cohesion of sandy soil and fine contents ratio.

Fine contents Ratio Fc(%)	10	25	40	50
Cohesion C'(kN/m2)	0.0	10.0	13.1	16.0

segment length, the monitored chamber pressure was smaller than digging phase and was used as the model pressure for the analysis.

Young's modulus is estimated as E=2800N(kN/m2), where N is a value of SPT, N for the ground and N=50 for the sand ground above the shield.

3D FEM simulation is performed for different parameters as shown in Table 3. The results for the Model F40C20 are shown in Figure 9. The yielding zone is mainly concentrated at the face and the horizontal displacement is concentrated at the center of the face. When the cohesion is greater than C≥10(kN/m2), the plastic deformation is stable. However, the cohesion is decreased to less than about C<10 (kN/m2), the plastic deformation becomes unstable, and the numerical solution was found to become uncontrolled condition of unlimited deformation. The plastic zones for C=10 (kN/m2) as stable and for C=7.5 (kN/m2) as unstable cases are shown I n Figure 10. As far as the plastics zones are concerned, the zones are rather limited very near the tunnel face, which is due to the confinement condition of the shield machine. The relationship between the cohesion of the sand layer and displacement is plotted in Figure 11.

Table 3. Ground property.

Model	E	ν	ϕ	C	dUy	stress state, stable or unstable
	(kN/m2)		(°)	(kN/m2)	(cm)	
Elastic	140,000	0.3		.	2.71	elastic
F40C40	140,000	0.3	40	40.0	4.90	plastic, stable deformation
F40C20	140,000	0.3	40	20.0	5.72	plastic, stable deformation
F40C10	140,000	0.3	40	10.0	12.5	plastic, stable deformation
F40C75	140,000	0.3	40	7.5	>24.5	plastic, unstable deformation
F40C05	140,000	0.3	40	5.0	>304.2	plastic, unstable deformation
F40C00	140,000	0.3	40	0.0	>500.	plastic, unstable deformation

In the zone of 200m from the face shown in Figure 8 and Table 2, the cohesion is expected as C=0.0. The face stability was anticipated as unstable and induced unlimited displacement for stopping phase.

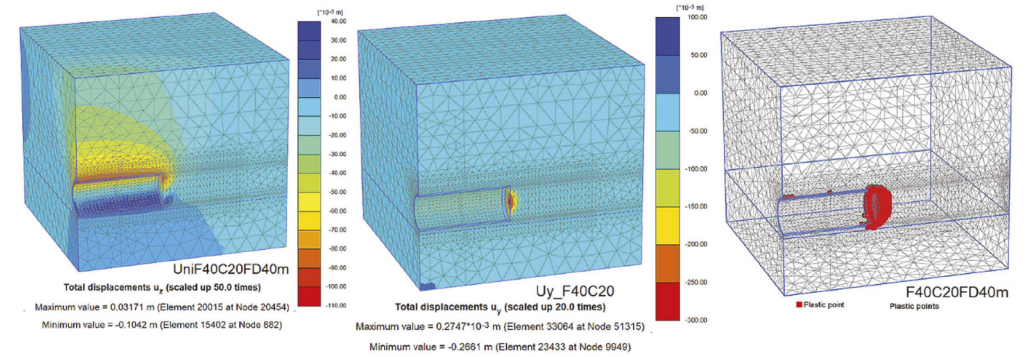

Vertical Displacement Horizontal Displacement Plastic Yielded Zone

Figure 9. Results of the simulation for F40C20.

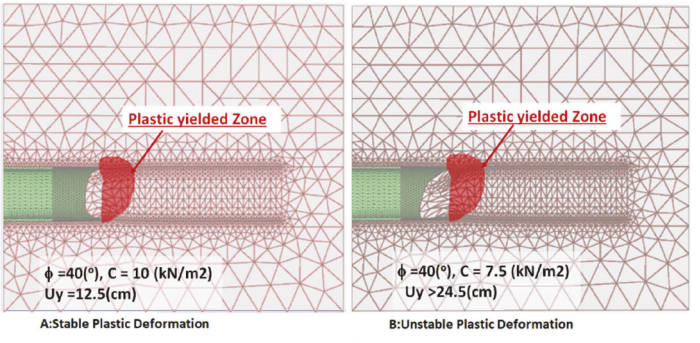

Figure 10. Stable and unstable yielded failure.

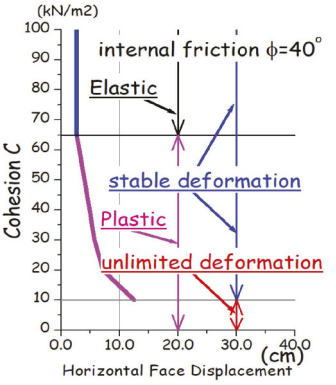

Figure 11. Face stability and cohesion.

Since no free space in front of the shield machine, the unstable plastic condition does not imply the direct failure of the face. However, Once the shield machine begins to dig, the rotation of cutting wheel easily allows for the plastic soil to come out without any control with water flow into the face, which finally results in loosening dense sand ground.

3 DIGITAL TWIN OBSERVATIONAL METHOD TO CONTROL FACE STABILITY

3.1 *Face loading/unloading tests*

To obtain proper chamber pressure for the site, face loading/unloading test may be performed. If displacement around face with changes of chamber pressure, possible sets of the geotechnical parameters of the ground can be estimated. Based upon these parameters, digital simulation can be performed and can be used to predict the shield tunnel performance. Digital observation of the shield tunneling shall be compared with digital simulation. A flow chart is shown in Figure 12 to show the general approach of the digital twin observational method to control face stability.

3.2 *Digital twin observational method*

One of the key factors for the face stability is to control the chamber pressure. Direct in-situ method and evaluation is proposed to obtain the appropriate range of the chamber pressure and to modify them by digital twin method of the Flow chart as shown in Figure 11.

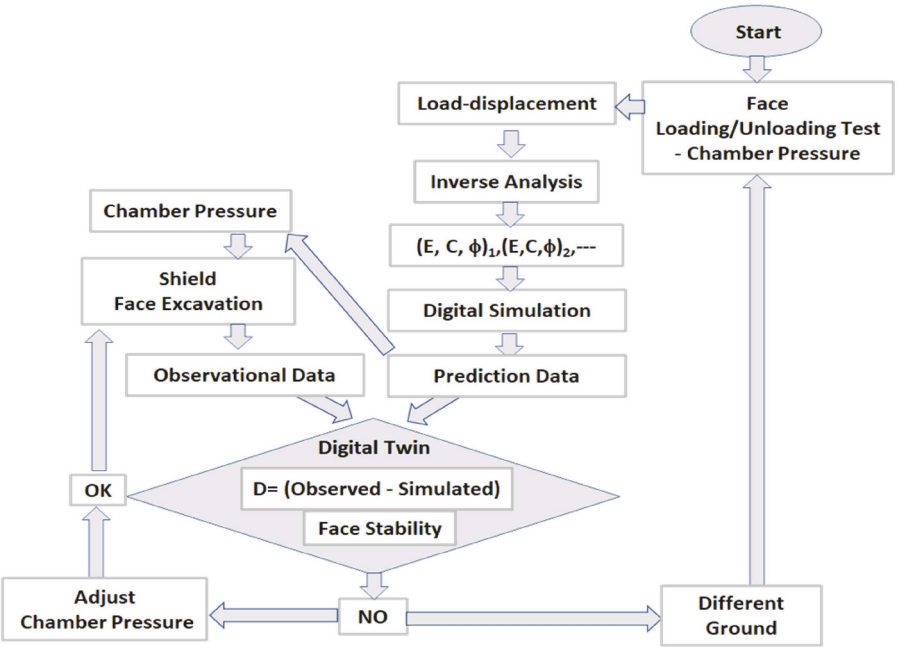

Figure 12. Flow chart of digital twin observational method.

4 CONCLUSIONS

Loosening of dense sand layer above shield tunneling for 200 m length is due to the strength characteristics of no cohesion which induced in unstable shield face and resulted in sink hole as well as caves underground. It may be estimated the appropriate range of the chamber pressure but it is much more practical and straight forwards to carry out face loading/unloading test at the site.

For the safety of face stability, digital twin observational method is proposed by face loading and face unloading tests to obtain the appropriate chamber pressure. Geotechnical parameters shall be obtained by inverse analysis for the tests and further used for simulation of tunnel performance in the next step with different boundary conditions.

REFERENCES

E-Nexco, 2020, https:www.e-nexco.jp/en/pressroom/kanto/2020/1018/00008605.html

Kim et.al, 2017, Effect of Fine Fraction Content in Soil Materials on Stability of River Dike, Ground and Construction, Vol.35, No.1, pp 37–44, Chugoku-Branch, JGS.

Hatanaka, M. et.al, 1999, Empirical Correlation between Internal Friction Angle and Normalized SPT value(N1) for Sandy Soils, Journal of Soils and Foundations, Vol.47-8 pp. 5–8, JGS.